

Defect Tolerance in as-deposited Selenium-alloyed Cadmium Telluride Solar Cells

Thomas A. M. Fiducia¹, Amit H. Munshi², Kurt Barth², Daniela Proprentner³, Geoffrey West³, Walajabad S. Sampath², and John M. Walls¹

¹Loughborough University, Loughborough, Leicestershire, LE11 3TU, United Kingdom

²Colorado State University, Fort Collins, Colorado, 80523, USA

³University of Warwick, Coventry, CV4 7AL, United Kingdom

Abstract — The efficiency of cadmium telluride (CdTe) solar cells is limited primarily by voltage, which is known to depend on the carrier concentration and carrier lifetimes within the absorber layer of the cell. Here, cathodoluminescence measurements are made on an as-deposited CdSeTe/CdTe solar cell that show that selenium alloyed CdTe material luminesces much more strongly than non-alloyed CdTe. This reduction in non-radiative recombination in the CdSeTe suggests that the selenium gives it a certain defect tolerance. This has implications for carrier lifetimes and voltages in cadmium telluride solar cells.

Index Terms — Cathodoluminescence, CdSeTe, charge carrier recombination, solar cell, voltage.

I. INTRODUCTION

The highest efficiency cadmium telluride solar cells contain a selenium-graded CdTe absorber [1][2]. While the selenium was first introduced to lower the material band gap and increase device current – to the expected detriment of voltage – it was found that cell voltages were unaffected by the lower band gap at the front of the absorber [1]. The high voltages were explained by the longer carrier lifetimes measured in the CdSeTe (CST) devices [3]. It was suggested that these were caused by: a) improved band alignments at the front interface; and/or b) grading of the absorber band gap effectively acting as an electron reflector. Here, cathodoluminescence data is presented that suggests that as well as potentially improving recombination behaviour at the device level as above (i.e. by changing band profiles along the depth of the device), selenium improves the intrinsic recombination properties of the semiconductor material at an atomic level, imbuing the material with a defect tolerance. This has important potential implications for device design and performance.

II. EXPERIMENTAL

A superstrate CST/CdTe device was fabricated by Close-space Sublimation (CSS) at Colorado State University, resulting in the device structure shown in Fig. 1. To make the cell stack, 100 nm of MgZnO was first sputtered onto a TCO-

coated glass substrate. This was followed by ~800 nm of CdSeTe and ~3 microns of non-alloyed CdTe, both deposited by CSS [4]. The CST layer has been measured to contain 10 at. % selenium [1]. The cell was left as-deposited to minimise any modification of the electronic properties of the materials by post-deposition treatments.

Following deposition of a protective layer of platinum a 7°, 30-micron wide bevel was milled through the device stack, as shown schematically in Fig. 1. This was performed in a Dualbeam SEM with a Ga ion beam at 30 kV, using a 0.5 nA final polish.

Panchromatic cathodoluminescence (CL) measurements were performed on the bevel in an SEM equipped with a parabolic mirror and a PMT detector. During the measurements a 7kV electron beam was rastered over the bevel while luminescence escaping the surface was collected by the mirror and fed to the detector. Secondary ion mass spectrometry (SIMS) maps on a different CdSeTe/CdTe bevel were collected at 10pA with a Hiden Energy Quadrupole SIMS system attached to a FEI Scios SEM-FIB.

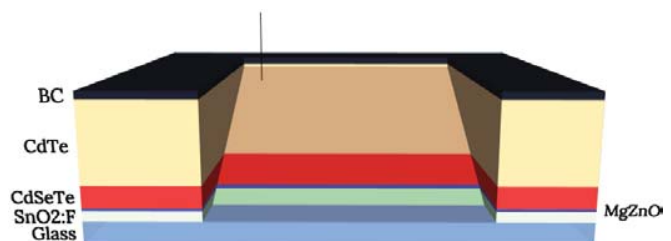


Fig. 1. Schematic of the CdSeTe/CdTe device structure and beveled surface. The bevel angle is 7° from the horizontal. Layer thicknesses are to scale apart from the glass and back contact (glass 3mm, SnO₂:F 400 nm, MZO 100 nm, CdSeTe ~1 μm, CdTe ~3 μm, BC 25 μm).

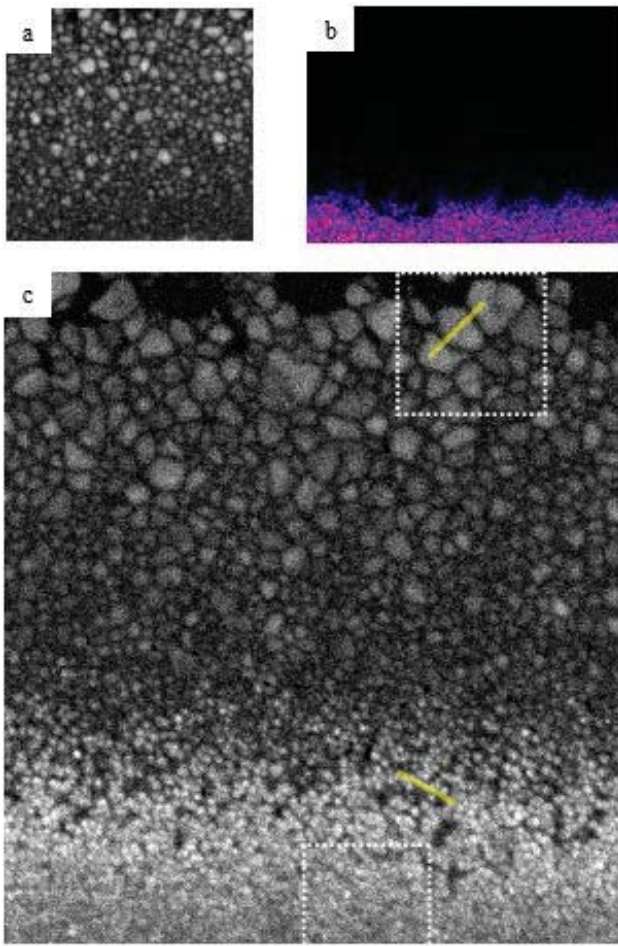


Fig. 2. (a) panchromatic CL image of a bevel on a normal CdTe absorber with no CST layer (for comparison with c). (b) SIMS map of selenium signal on an untreated CST/CdTe bevel. (c) panchromatic CL image of a 7° bevel on a CST/CdTe device. F.O.V 28 x 30 μm . The boxes designate higher magnification areas shown in Fig. 4. The lines show regions used to create profiles in Fig. 3.

III. RESULTS AND DISCUSSION

A panchromatic CL image from the bevel is shown in figure 2 (c). Dark contrast is seen at the grain boundaries in the upper region of the bevel (the CdTe layer). This observation is consistent with previous CL measurements on non-alloyed CdTe devices and demonstrates that the grain boundaries act as recombination centres [5]. The behavior can be seen more clearly in the higher magnification image in Fig. 4 (a). In addition to the images, the CdTe line profile in Fig. 3 shows a clear V-shaped drop in the CL signal at grain boundaries.

As well as drops in signal at the grain boundaries in the CdTe layer, the images show that there are grain to grain variations in CL signal in the CdTe that are not dependent simply on grain size. Reasons why this variation may occur

include: 1) differences in the subsurface grain boundary behaviour (unseen boundaries just below the surface may affect carrier recombination and therefore the CL signal); 2) grain-to-grain variations in the chemistry or point defects in the material, leading to differences in the density of active trap states and hence luminescence; and 3) differences in the crystal plane that is exposed at the surface of the bevel for different grains (111, 112, etc). There is some evidence in the high magnification image in Fig. 4 (a) that suggests that the third reason, exposure of different crystal planes, plays an important role in the signal variations. The image shows changes in the CL signal across $\Sigma 3$ (111) twin boundaries (arrowed in the secondary electron image in part (b) of the figure). Neither point defects nor sub-surface GBs are likely to vary between twinned crystals in this way. However, the crystal plane that grains terminate in varies either side of a $\Sigma 3$ (111) twin. This therefore seems the most likely reason for the grain-to-grain signal variations seen in the twinned grains and the rest of the data (in addition to variations due to grain size). Figure 5 shows an example of how this might occur either side of twins, as well as either side of a general grain boundary. Grain 2 in the schematic terminates in a (111) crystal plane. However in the adjacent grains (1 and 3) the crystal orientation has been rotated 180 degrees about the $\langle 111 \rangle$ direction, and so they terminate in a different crystal plane. This would likely result in differences in the type and density of defects at the surface and hence affect the amount of non-radiative recombination and CL signal from each side of the boundary. Grains either side of a general GB, like grains 3 and 4 in the figure, can have any orientation relative to one another and so can clearly often terminate in different crystal planes with different defect properties. One way to establish the extent to which different surfaces cause CL signal variations would be to perform CL measurements at higher beam

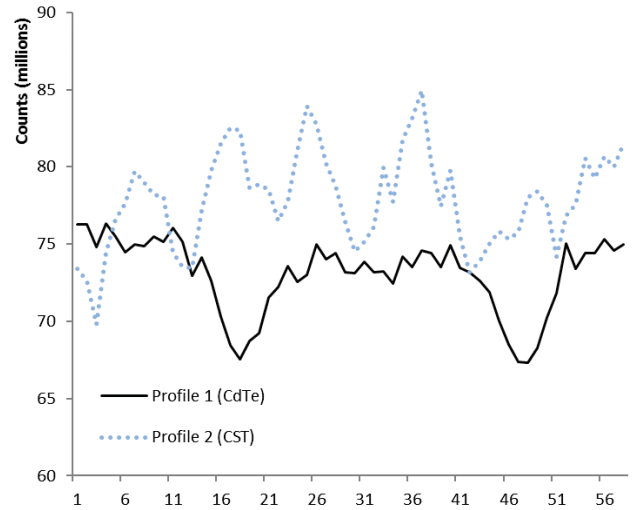


Fig. 3. CL intensity line profiles in the CdTe and CST regions of the bevel shown in Fig. 2.

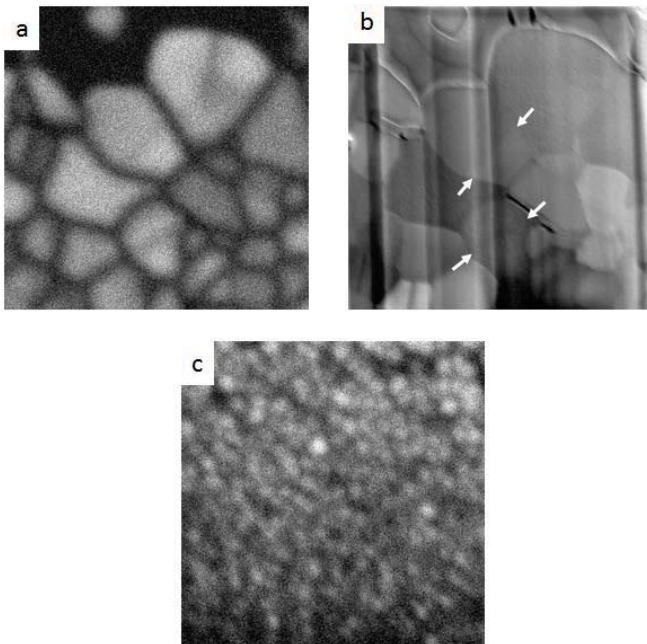


Fig. 4. (a) High magnification panchromatic CL image of the CdTe region of the bevel. The F.O.V is $6.5 \times 6.5 \mu\text{m}$. position on the bevel is shown by box 1 in figure 2 (c). (b) Accompanying secondary electron image of the area shown in (a), with arrows highlighting lamellar twins. (c) High magnification panchromatic CL image of the CdSeTe region of the bevel.

energies and determine if the magnitude of the variations decreases. These results highlight the potentially important role that the measurement surface plays in interpretation of low beam energy CL measurements.

Deeper in the CdTe layer, towards the centre of the bevel, the CL signal decreases as the CdTe grains get smaller. This is expected, as smaller grains mean that even when the electron beam is in the middle of a grain, generated carriers are likely to be within a diffusion length of a grain boundary.

At the very bottom of the bevel, the CL signal is very bright (average signal in the region is around 350,000 counts,

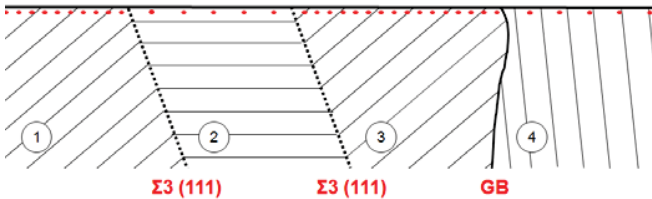


Fig. 5. Schematic showing how different grain orientations in polycrystalline CdTe might give rise to different densities of harmful defects on the surface of the material and hence affect CL intensities. Two $\Sigma 3$ (111) twins and a general grain boundary (GB) are shown. Red dots represent surface defects. In grain 2 the (111) crystal plane is exposed at the CdTe surface.

compared to 15,000 in the upper part of the bevel). This corresponds to the CST layer, where the SIMS map (Fig. 2 (b)) shows that selenium is present, and where the collected CL spectra show a clear shift to a longer wavelength luminescence (the peak in the bright region is at around 860 nm, compared to 820 nm in the upper region of the bevel, see Fig 6). This brighter luminescence, which occurs despite the small grain sizes in the region, suggests that the CST material has a significantly higher overall luminescence efficiency than the CdTe (meaning that there is less defect-mediated non-radiative recombination of carriers in the CST). The effect has been seen in multiple samples and measured in different CL systems. In addition, possible artefacts relating to the detector efficiency in different wavelengths in the spectrum have been ruled out.

The higher magnification image of the CST region in Fig 4 (b) shows that just like in the CdTe, there is darker contrast at the grain boundaries in the material. However, unlike the large-grained CdTe region at the top of the bevel, the CL signal does not plateau in the grain interiors (see line profile 2 in figure 3). This implies that the GI CL signal has not reached its maximum, because even in the middle of the grain there is still some recombination occurring at grain boundaries. From the figure it is clear that even with some grain boundary recombination, the CST grain interior signal is higher than the plateaued grain interior signal from the CdTe (note that the grains chosen for the CdTe line profile are among the brightest in the CdTe material). This implies that selenium reduces non-radiative recombination in the grain bulk of the material. In other words, there is an active defect in the untreated CdTe material that is to some extent pacified by the presence of ~ 10 at.% selenium. This poses certain questions such as: 1) whether different percentages of selenium alloying would have a similar, or perhaps even more pronounced effect on defect passivation in the material, 2) whether the selenium pacifies

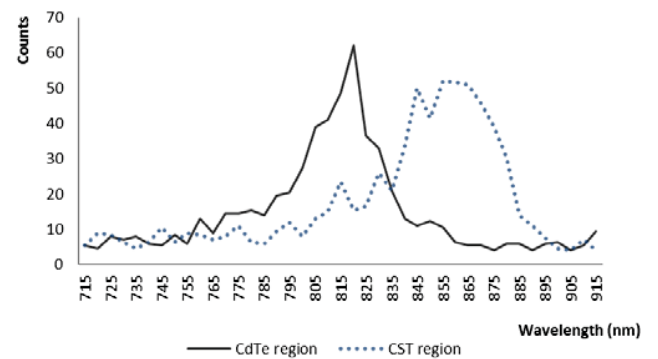


Fig. 6. CL spectra taken in the CdTe and CST regions showing a shift in peak wavelength emissions between the two materials. Areas of the bevel over which the spectra were taken are different dimensions, so the integrated areas under the curves – giving total luminescence in that region – are not directly comparable.

grain boundaries and other extended defects, and 3) whether selenium improves recombination properties in cadmium chloride treated CST material.

IV. CONCLUSIONS

Cathodoluminescence measurements have been performed on an untreated CdSeTe/CdTe solar cell in order to determine the origin of higher than expected carrier lifetimes and voltages in CdSeTe-based solar cells. The luminescence signal is found to be significantly higher in the CdSeTe material than in CdTe, implying that selenium passivates defects in the grain bulk, and perhaps grain boundaries of untreated CdTe material. This raises the prospect that carrier lifetimes and voltages in CdTe solar cells can be further improved by optimization of the selenium content and grading within the device. In addition, the crystal plane that is present at a surface appears to have a significant effect on the CL signal measured at the surface.

ACKNOWLEDGEMENTS

The author would like to thank Dr. Budhika Mendis of Durham University for help with data interpretation and Dr Richard Beanland for the use of CL equipment at Warwick University. Focused Ion Beam milling was performed using equipment at the Loughborough Materials Characterisation

Centre. The authors at CSU are thankful for funding support from NSFs Accelerating Innovation Research and NSFs Industry/University Cooperative Research Center programs.

REFERENCES

- [1] A. H. Munshi, J. Kephart, A. Abbas, J. Raguse, J. Beaudry, K. Barth, J. Sites, J. Walls, and W. Sampath, “Polycrystalline CdSeTe / CdTe Absorber Cells With 28 mA/cm² Short-Circuit Current,” pp. 1–5, 2017.
- [2] D. E. Swanson, J. R. Sites, and W. S. Sampath, “Co-sublimation of CdSe x Te 1 Å x layers for CdTe solar cells,” *Sol. Energy Mater. Sol. Cells*, vol. 159, pp. 389–394, 2017.
- [3] J. M. Kephart, A. Kindvall, D. Williams, D. Kuciauskas, P. Dippo, A. Munshi, and W. S. Sampath, “Sputter-Deposited Oxides for Interface Passivation of CdTe Photovoltaics,” *IEEE J. Photovoltaics*, pp. 1–7, 2018.
- [4] D. E. Swanson, J. M. Kephart, P. S. Kobyakov, K. Walters, K. C. Cameron, K. L. Barth, W. S. Sampath, J. Drayton, and J. R. Sites, “Single vacuum chamber with multiple close space sublimation sources to fabricate CdTe solar cells,” *J. Vac. Sci. Technol. A Vacuum, Surfaces, Film.*, vol. 34, no. 2, p. 021202, 2016.
- [5] J. Moseley, W. K. Metzger, H. R. Moutinho, N. Paudel, H. L. Guthrey, Y. Yan, R. K. Ahrenkiel, and M. M. Al-jassim, “Recombination by grain-boundary type in CdTe,” *J. Appl. Phys.*, vol. 118, 2015.